CONF-800204--3

LA-UR-79-3110

TITLE: PERMEABILITY ENCHANCEMENT USING EXPLOSIVE TECHNIQUES

AUTHOR(S): T. F. Adams, S. C. Schmidt, and W. J. Carter

SUBMITTED TO: 1980 Energy Sources Technology Conference
and Exhibition, New Orleans, LA,
February 3-7, 1980

MASTER

University of California

LOS ALAMOS SCIENTIFIC LABORATORY
Post Office Box 1663 Los Alamos, New Mexico 87545
An Affirmative Action/Equal Opportunity Employer

Form No. 836 R3
St. No. 2629
12/78

UNITED STATES
DEPARTMENT OF ENERGY
CONTRACT W-7405-ENG. 36

PERMEABILITY ENHANCEMENT USING EXPLOSIVE TECHNIQUES

by

T. F. Adams
S. C. Schmidt
W. J. Carter

Staff Members
University of California
Los Alamos Scientific Laboratory
Los Alamos, NM 87545

ABSTRACT

In situ recovery methods for many of our hydrocarbon and mineral resources depend on the ability to create or enhance permeability in the resource bed to allow uniform and predictable flow. To meet this need, a new branch of geomechanics devoted to computer prediction of explosive rock breakage and permeability enhancement has developed. The computer is used to solve the non-linear equations of compressible flow, with the explosive behavior and constitutive properties of the medium providing the initial/boundary conditions and material response. Once the resulting computational tool has been verified and calibrated with appropriate large-scale field tests, it can be used to develop and optimize commercially useful explosive techniques for *in situ* resource recovery.

NOMENCLATURE

I = internal energy per unit mass, J/kg

P = pressure, GPa

t = time, s

u = velocity, m/s

ρ = mass density, Mg/m^3

SUPERSCRIPTS

$\rightarrow$ vector

INTRODUCTION

Explosives have played a role in georesource recovery since at least 1705 in the United States, and since the early 1600's in Europe (1). However, until recently it has not generally been necessary to exercise great control over explosive events in rocks since chemical processing has always been done above ground. With the emergence of *in situ* processes for extraction of energy and mineral resources, this picture has changed. There is now a need for a more controlled predictive dynamic fragmentation or fracture capability so that the desired permeability and fluid flow through the resource bed can be achieved. Only then can we hope to optimize both technically and economically the preparation of *in situ* leach or solution mines for copper, uranium, or other materials, and stimulation from a well-bore of oil, gas, or geothermal resources in low-permeability reservoirs.

Although the processing requirements for each of these diverse operations are quite different, the underlying theory and approach for preparation of the resource bed is basically the same. Clearly a generalized approach which accounts for site-specific geology and geometry to predict reactive multi-phase fluid flow in the resource bed as a result of blasting is required. The development of large digital computers over the past few years has made such an approach possible. A new branch of geomechanics, devoted to the computer prediction of fracture patterns, void distributions, particle size distributions, and flow path permeabilities resulting from explosive loading is emerging. The techniques are centered around numerical solutions of the equations of compressible flow using appropriate boundary conditions and material constitutive relations. This approach requires beyond the state-of-the-art laboratory studies to determine the dynamic response of geophysical materials for a wide variety of *in situ* conditions and large-scale field tests to establish confidence in the predictive capabilities developed.

THEORY

The first, most dramatic effect of blasting in rock is the generation of an intense stress wave. The propagation of the stress wave is governed by the principles of the conservation of mass, momentum, and energy. These fundamental principles may be written mathematically in the form of a set of coupled partial differential equations (2). For a fluid, these equations are, respectively:

$$\frac{\partial \rho}{\partial t} + \vec{\nabla} \cdot (\rho \vec{u}) = 0, \tag{1}$$

$$\frac{\partial \vec{u}}{\partial t} + (\vec{u} \cdot \vec{\nabla}) \vec{u} + \frac{1}{\rho} \vec{\nabla} P = 0, \tag{2}$$

$$\frac{\partial}{\partial t}\left(I + \frac{1}{2}u^2\right) + (\vec{u}\cdot\vec{\nabla})\left(I + \frac{1}{2}u^2\right) + \frac{1}{\rho}\vec{\nabla}\cdot(P\vec{u}) = 0. \qquad (3)$$

For a material with strength, such as rock, the pressure terms in equations (2) and (3) would be replaced with analogous terms involving the general stress tensor.

These equations must be augmented with "constitutive relations," which give the stress and internal energy as functions of the current state and previous strain history of the rock. In general, constitutive relations would include effects such as viscoelasticity, plasticity, and fracture. In practice, elastic/plastic and fracture effects are so different in character that they are usually treated separately. They will be discussed separately in some depth below in view of the critical roles they play in the results of blasting.

Given the constitutive relations, equations (1), (2), and (3) are predictive in the sense that the effects of the blast are uniquely determined by the initial and boundary conditions. In this context, we can consider the energy and momentum input from the explosive itself as a combined initial/boundary condition. The explosive provides the initial impulse that generates the stress wave and then maintains a high residual pressure in the borehole. At late times, the gases produced by the explosive play a somewhat different role as they spread through the broken rock and act to "heave" the rubble. The characterization of explosive behavior will be discussed in more detail below as it plays a central role in the effort to model the effects of blasting.

The behavior of the explosive is complex, and the constitutive relations are highly non-linear. We therefore have a set of difficult non-linear partial differential equations to solve. These equations have analytic solutions only for the simplest, most highly idealized situations. The solutions we must seek are therefore numerical ones obtained with sophisticated large-scale computers. Indeed, the complexity of these equations has provided much of the impetus for the development of larger, faster computers by the scientific community over the past several decades.

The basic partial differential equations must be rewritten via one of several approximation schemes before a solution is possible. Once this is done, the solutions to the equations may be obtained in a step-by-step fashion at successively later times after the initial detonation. These solutions are obtained at a large number of discrete mesh points spread throughout the region of interest around the charges. To model a realistic field size blast may require a mesh with tens of thousands of points and may involve integration over thousands of time steps. Deck-loaded charges with delays between the firing of the various decks can be taken into account during the calculations.

EXPLOSIVE CHARACTERIZATION

Quantitative characterization of the performance of commercial blasting agents (non-ideal explosives) is crucial to the success of a computer-designed fragmentation or permeability enhancement scheme, since the explosive provides the initial and boundary conditions for the basic equations. If the rock response characteristics are sufficiently well known, the calculations can provide guidance for tailoring, or chemical modification, of the explosive for optimum breakage efficiency.

An "ideal" explosive is one in which the chemical reactions run to completion at or very close to the detonation front. The behavior of an ideal explosive depends very little on the charge diameter, confinement, or booster system. In contrast, a "non-ideal" explosive is one in which there is significant delayed reaction of at least some components. The behavior of a non-ideal explosive as reflected for example in the detonation velocity and peak (C-J) pressure, may depend sensitively on the geometry and method of initiation. The distinction is a technical one; non-ideal explosives may be more suitable for field applications, such as fracturing oil shale or coal, or for well stimulation.

Considerable work has been done at the Los Alamos Scientific Laboratory on ideal explosives, since military explosives are usually of this type. Recently, this work has been extended in an effort to characterize commercial, non-ideal explosives, such as ANFO (3). To date, the focus has been on studying the early-time behavior of the explosive to determine the detonation velocity, C-J density and pressure, and equation-of-state for the reaction products. Work is in progress to study the late-time gas effects produced by these explosives.

The characterization of an explosive is a three-step process. First, a chemistry code is used to predict the ideal behavior of the explosive from its composition. Then, field tests are conducted, where the explosive is detonated under controlled conditions, so that its actual behavior can be studied. Finally, the partial reaction of the explosive is taken into account in the chemistry code so as to give agreement with the field data. Fig. 1 shows a comparison between the calculated and observed behavior for 0.1 m diameter ANFO. The end products, which are input to the stress wave propagation code, are the detonation velocity, conditions at the C-J point, and the variation of the pressure and energy as the reaction product gases expand and cool. The technical aspects of numerical modeling of explosives are described in a book by Mader (4).

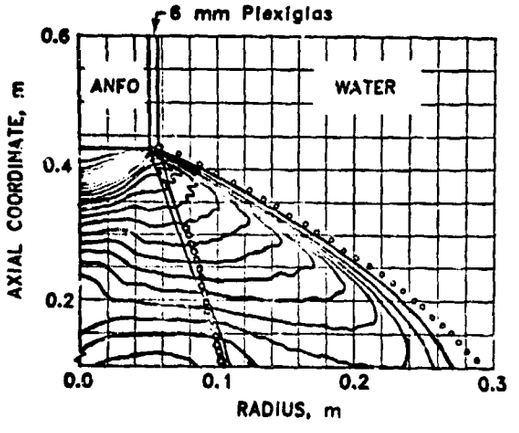

Fig. 1 Comparison of calculated and observed shock and Plexiglas-water interface positions during detonation of 0.1 m diameter ANFO. The open circles are the observed points. The contours are calculated pressure at 0.1 GPa intervals. The non-ideal behavior of the ANFO has been modeled by assuming that 55 percent of the ammonium nitrate undergoes delayed reaction behind the detonation front (see 3).

The ability to characterize explosives is the first step toward the modification of explosives to better meet engineering goals. Such tailoring could include changes in detonation velocity, C-J pressure, total energy, and control of rise time and pulse duration. Changes could be made to do more than optimize breakage. For example, it might be desirable to tailor the explosive to limit the production of fines near the borehole. Obviously, the coupling of the detonation energy to the rock and the dynamic response of the rock itself are important considerations in explosive tailoring, and the choice of explosive must be specific to the reservoir bed.

CONSTITUTIVE RELATIONS

The constitutive relations important in *in situ* processing applications must describe the dynamic response of geologic materials under a wide variety of conditions. Historically, laboratory investigations of rocks have concentrated on measuring a limited number of properties under very restricted conditions. For example, yield strength and some of the elastic moduli have been measured, but usually at ambient temperature, low pressure, and at fixed strain rate. While necessary for a complete material description, these data are not sufficient to describe the response to dynamic loading. The effects of such parameters as loading rate, pore pressure, elevated temperatures and pressures, and the presence of natural joints and fractures must all be included. No geologic material has yet been studied sufficiently to allow an unambiguous calculation of the breakage pattern and permeability distribution resulting from a given explosive loading. There has, however, been a considerable amount of work done on a few materials of interest, including Green River oil shale (5, 6, 7), Antrim shales (8), and Devonian gas shales (9). These measurements have contributed to simplified constitutive relations, thus allowing rudimentary solutions to the stress-wave propagation equations for dynamic fracture applications.

Constitutive relations, in general, express the response of a material to a given driving mechanism. For the geologic materials considered in dynamic fragmentation applications, the response will vary considerably as the loading rate and the material constraints change. Since both effects are important, for an *in situ* explosive event, several different experimental techniques are required to determine the applicable constitutive relations.

Experience has shown that many material properties for shales can be correlated with initial density or kerogen content (10). This is particularly valuable for computational purposes. Elastic moduli of oil (11) and gas (12) shales have been determined as a function of density at zero confining pressure. The ultrasonic sound speed data used to determine these moduli for Green River oil shale are shown in Fig. 2. The moduli are obtained from the velocity data using standard theoretical relations, assuming that the material is transversely isotropic. (Actually, there is some evidence that these materials are not strictly transversely isotropic (11).

In the ultrasonic measurements, porosity was carefully avoided so that a correlation between sound speed and density could be established. The effects that porosity and water saturation can have on the sound speed and the moduli have been demonstrated by measurements on a highly porous (12 per cent), low kerogen content oil shale from the Anvil Points Mine. The sound speeds were determined for samples both dry and saturated with water. The sound speed data are summarized in Table I. The sound speeds given there for the nonporous material were determined from the velocity fits given in Fig. 2 using the densities of the mineral material and kerogen alone.

The data in Table I show that the 12 per cent porosity appears to have lowered the velocities by 14-23 percent. Filling the pores with water further lowered the longitudinal velocities by 10 per cent and the shear velocities by 20 per cent. The requirement to make accurate assessments of the effects of kerogen content, porosity, and saturation levels is clearly evident from these measurements.

A constitutive relation necessary for fragmentation calculations is the material failure envelope, i.e., the limits to which the material can be loaded before it fails, and the resulting residual material

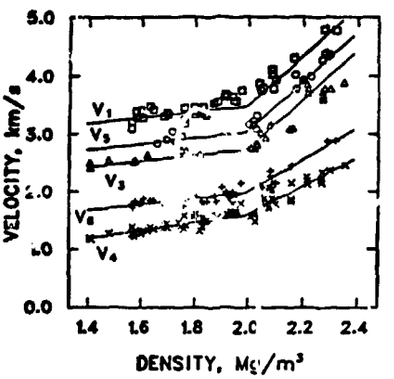

Fig. 2 Velocities of five propagation modes versus density for Green River oil shale. The data and solid line fits are labeled according to mode as follows: V_1 (squares), longitudinal (parallel to bedding); V_3 (triangles), longitudinal (perpendicular to bedding); V_4 (crosses), shear (perpendicular to bedding, particle motion parallel to bedding); V_5 (circles), quasi-longitudinal (45° to bedding); V_6 (plus signs), shear parallel to bedding, particle motion parallel to bedding).

TABLE I

VELOCITIES OF FIVE PROPAGATION MODES IN OIL SHALE WITH DIFFERENT POROSITY/SATURATION

Mode	Velocity, km/s		
	Nonporous	Dry	Saturated
longitudinal (parallel to bedding)	5.60	4.44	4.01
longitudinal (perpendicular to bedding)	4.85	4.03	3.66
shear (perpendicular to bedding, particle motion parallel to bedding)	2.88	2.47	1.99
quasi-longitudinal (45° to bedding)	5.15	4.28	3.90
shear (parallel to bedding, particle motion parallel to bedding)	3.41	2.61	2.15

properties after failure. Yield strengths have been measured as a function of density and mean stress (7). These results, including the shift in the brittle/ductile transition can be seen in Fig. 3. Rate dependence and failure properties based on these data have been incorporated into a scalar damage model (13). Fragmentation calculations based on this model have been moderately successful.

Intermediate and high strain rate experiments are most conveniently done in plane geometry using wave propagation techniques. For strain rates above 10^4/s, dynamic properties can be measured using a gas-driven gun or explosive loading device. A schematic drawing of a laboratory-scale gas gun is shown in Fig. 4.

Plate impact devices can be used for a variety of experiments. Much useful information is contained in plots of shock velocity or wave speed versus particle velocity. Such a plot for a Devonian shale, obtained with a standard technique called the "impedance match method" (14), is shown in Fig. 5. Plots like this one have been used to derive the equilibrium Hugoniot equation-of-state for oil and gas shales (5, 12).

An important feature of the example shown in Fig. 5 is the phase transition that occurs in this gas shale at a pressure of approximately 20 GPa at this loading rate. This is deduced from the offset in the plot at a shock velocity of about 6 km/s. The actual physical mechanisms governing the transition are not known, but it is suspected that the behavior is due to the α-quartz-to-stishovite phase transformation. This is probably the explanation, even though the transition pressure found here is 6-10 GPa larger than the static stishovite transition pressure. Meaningful constitutive relations must include this transition, not only to describe the wave propagation properly, but also because the material could absorb large amounts of energy during the transformation. Understanding this phenomenon becomes particularly important in the design of practical devices such as jet penetrators.

The effect of loading rate on the yield surface can be seen from the results, illustrated in Figs. 6a and 6b, of a second type of high strain rate experiment (6). Here manganin gauges are embedded within a sample of oil shale and the stress-time profile is monitored while the sample is hit with a high-velocity projectile. These profiles, shown in Fig. 6a, are transformed to the more usual stress-strain contours, which are shown in Fig. 6b. From the successive gauge records in Fig. 6a, the dispersion of the shock profiles is evident as the stress rise times increase with distance. This dispersion indicates that the shale yields gradually under compression. This is also evident from the curvature of the stress-strain plot. When compared with Fig. 3, however, the effect of increased loading rate is obvious. Where statically, shale could only support a 0.1 GPa load at zero confining pressure before yielding, the dynamic results show considerably greater strengths. Again, the constitutive relations to be used for numerical calculation of stress wave propagation must account for this behavior.

The most difficult loading regi to deal with is the intermediate strain rate region. Part of the problem of obtaining accurate material behavior and constitutive relations at the 10^1-10^3/s rates is the

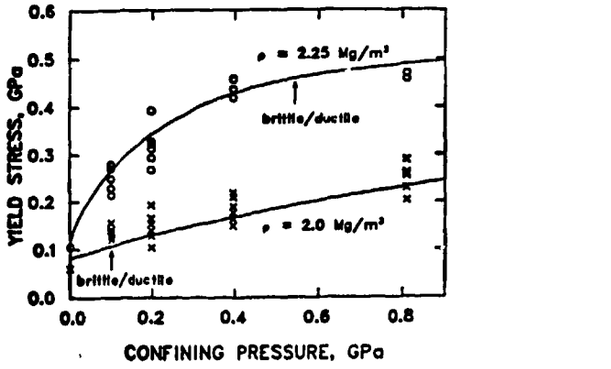

Fig. 3 Yield stress versus confining pressure for oil shale of two different densities. The fits to the data are labeled with the oil shale density. The 2.25 Mg/m^3 oil shale (circles) is a moderate grade; the 2.0 Mg/m^3 oil shale (crosses) is rather rich in kerogen. The brittle/ductile transition points are marked with arrows. Note that the brittle/ductile transition occurs at a much lower stress level for the rich oil shale.

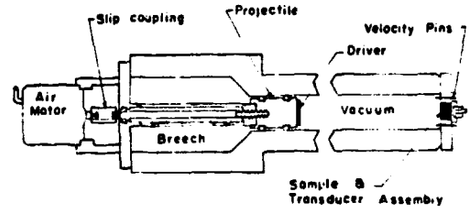

Fig. 4 Schematic drawing of a laboratory-scale gas gun. The driver is fired through the barrel toward the sample and transducer assembly at the right.

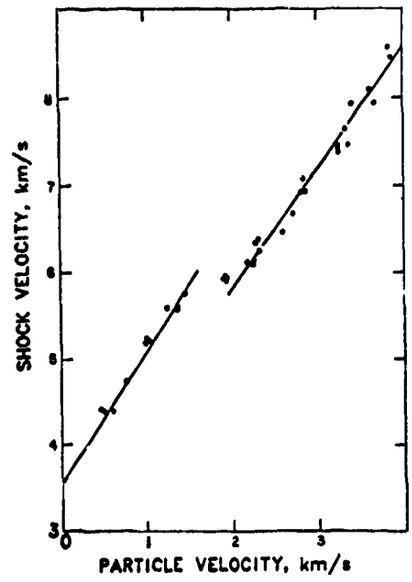

Fig. 5 Shock velocity versus particle velocity for Devonian gas shale. The discontinuity in the data at a shock velocity of about 6 km/s is related to a phase transition that occurs in the samples at this stress loading level.

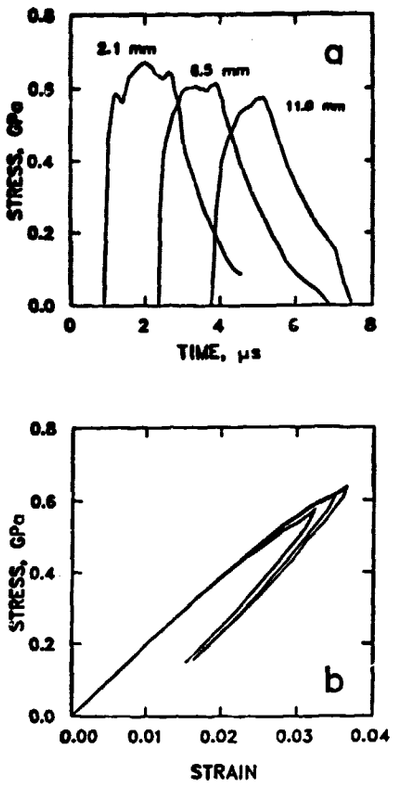

Fig. 6 Stress data obtained from gauges embedded in a sample of 2.08 Mg/m^3-density oil shale following impact by a high-velocity projectile. Fig. 6a shows stress versus time as reported by gauges at depths of 2.1, 6.5, and 11.0 mm. Note how the stress rise times lengthen as the shock propagates through the sample. Fig. 6b shows the stress-strain curves for each of the gauge locations. The strain rates are approximately 3×10^5/s loading and -1×10^4/s unloading. Note that the sample is loaded to nearly 0.6 GPa in this experiment, even though the static yield stress is approximately 0.1 GPa (cf. Fig. 3).

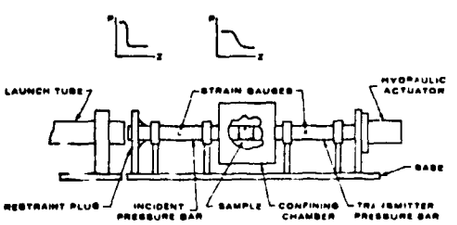

Fig. 7 Schematic drawing of a split-Hopkinson bar. A projectile is fired from the left to impact the incident pressure bar. This generates a stress wave, which propagates down the bar to the right to impact the sample in the confining chamber. The bar acts to disperse the pulse and reduce the strain rate at the sample. Illustrations of the pulse shapes at the left end of the bar and at the sample are shown in plots at the top of the figure. A portion of the pulse is transmitted through the sample to the right into the transmitter pressure bar.

extreme difficulty of performing suitable experiments. Split-Hopkinson bars (Fig. 7) or torsion bars can yield data up to about 10^3/s, although considerable uncertainty exists regarding the interpretation of data obtained from these experiments (15). Other experiments (16) have shown the need for adequate sample size and homogeneity. These data are essential for determination of the far-field behavior several borehole diameters removed from an explosive event. It is in this sub-kilobar pressure range and 10^2-10^3/s strain rate regime where much of the rock damage occurs.

A good start has been made toward gaining a fundamental understanding of the dynamic properties of geological materials important in *in situ* applications. At the same time, it is clear that effects such as pore pressure, elevated pressure and temperature, and material microstructure need to be explored in much greater depth so that meaningful constitutive relations can be developed. As a first step, we can expect to see in the near future a significant improvement in our understanding of the role played by strain rate effects.

FRACTURE MODELS

Geologic materials behave to some extent like elastic/plastic solids. At high pressure they exhibit ductile flow; however, at lower pressure they behave like brittle materials that may be fractured and can fail catastrophically under intense stress loading. The dynamic response of rock to low and moderate stresses is embodied in the usual constitutive relation, while the fracture process is generally treated by means of separate fracture models.

Fracture models may generally be divided into two categories: empirical statistical models and theoretical fracture mechanics models. The empirical statistical models have been reviewed by Kuznetsov and Faddeenkov (17). Theoretical fracture

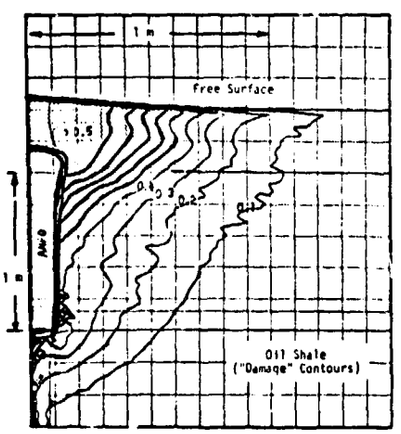

Fig. 8 Results of a computer simulation of the detonation in oil shale of a 1 m charge of ANFO (0.12 m in diameter), with the top of charge 0.4 m below the free surface. The contours show that regions of successively greater "damage," as calculated with the fracture model developed by Johnson (13). The shaded-in area (damage greater than 0.5) shows roughly the volume of the crater to be expected from this blast.

mechanics models are more appropriate for our purposes because they reflect both the microphysics of fracture and the strain history of the rock.

Several theoretical models for fracture under dynamic loading have been developed. One of the simplest is a direct extension of elastic/plastic theory, where the accumulated plastic strain is taken as a measure of fracture (18). This is clearly inadequate since the deformation of geologic materials during fracture is quite unlike ordinary plastic flow. The ductile flow of rock at high pressure may be the only characteristic of rock that closely resembles plasticity.

Johnson (13) has also developed a fracture model based on plasticity, but has built into it several features that more closely describe the behavior of rock. First, he introduces a "damage parameter," which varies from 0 to 1 as the rock is increasingly more heavily broken. The damage parameter is not plastic strain per se, but the damage is assumed to increase whenever the yield surface is crossed. The growth of damage is modeled in a rate-dependent fashion with a suitable time constant, and the growth law allows for the fact that it is harder to increase the level of damage in rock that is already heavily damaged. Effects of dilatancy are also included. Finally, there is some feedback as the increase in damage is taken to lower the yield strength of the rock, and thereby its resistance to shear deformation. Results of a stress-wave calculation based using this model are shown in Fig. 8. The most significant drawback of the damage model is that it is a scalar model, while real fracture has a strongly directional character. In addition, the model allows only in the simplest way for the effects of extensive fracture on the response of the material to successive loading. This means that the treatment of stress wave propagation through partially broken rock is not very satisfactory.

A somewhat more sophisticated fracture model has been developed by Grady and Kipp (19). In their model, the damage parameter represents a measure of the fracture-induced void volume in the rock. The rate at which the damage grows is determined by following the growth in void volume as applied stresses cause a statistical distribution of flaws to activate and grow. The incremental stress-strain relation is modified by the presence and the growth of damage. As a result, stress relaxation and energy dissipation associated with fracture effectively reduce the elastic moduli. This model is more satisfactory for treating the propagation of stress waves through broken rock, but it still has the limitation that it is a scalar model. Only a tensor model can properly account for the directional nature of fracture and fracture-induced stress relaxation.

A tensor mode, the "NAG/FRAG" ("nucleation and growth--with resulting fragmentation") model, has been developed at SRI International (20). This model has many of the features needed for a comprehensive three-dimensional fracture model. It is based on theoretical fracture mechanics, but it has built into it the experience gained in a series of laboratory explosive tests conducted on oil shale samples at SRI. The NAG/FRAG model has one principal weakness: it is formulated in terms of a number of adjustable free parameters. While the parameters could be determined empirically in principal, in practice it would be difficult to do so with a limited number of experiments.

A new tensor fracture mode, the "SCM" ("statistical crack mechanics") model, is being developed by J. K. Dienes and L. G. Margolin (21) at the Los Alamos Scientific Laboratory. This model is based on the analytic solution for the response of a penny-shaped crack to a general state of stress. The bulk response of the material is then obtained by superimposing a statistical distribution of cracks with various sizes and orientations. The distribution of cracks evolves with time as applied tensions and shears cause cracks to grow. It is still a bulk theory in the sense that the collective effect of many cracks is considered, rather than the growth of a single crack. However, it has all the desirable features of a tensor theory. Because it is based on rigorous microscopic theory, the SCM model involves on a small number of physically meaningful parameters, each of which could be determined in the laboratory or in a small number of field tests.

FLOW MODELING

The relation between fluid flow and fracture for a porous geologic material is by no means clear. No complete theoretical analysis exists for flow through a hydraulically- or explosively-produced fracture system. Yet for many applications, permeability, not fracture, is the crucial parameter. This is certainly the case for modeling flow in oil, gas, geothermal steam, and hot dry rock reservoirs, as well as for developing *in situ* oil shale, tar sands, and coal resource recovery techniques.

Several theories exist linking permeability to fracture. All of them recognize the importance of porosity, whether resulting from dilatation or present before the stimulation treatment, as the controlling factor. These theories are semiquantitative at best, and much more theoretical and experimental work relating rock deformation and fracture to permeability must be done. The importance of the "stress cage" (the compacted zone surrounding a borehole or fracture that restricts the flow) has been recognized for at least 15 years, but no quantitative data or theories that could mitigate its effects are available. Correlations between field-scale and laboratory data are perhaps more important for this branch of rock physics, since large-scale flow can be completely dominated by natural fractures and joints, which are carefully excluded in laboratory tests.

A promising start toward treating this very complex problem has been made using geomedia fluid flow models developed at the Los Alamos Scientific Laboratory. Historically, flow models have been limited to applications in uniform porous media. The new time-dependent models not only describe flow in fractured porous media, but also include the effects of diffusion and dispersion, heat exchange, sources and sinks, spatially varying material properties, and multi-component and multi-phase flow. These models are implemented in several large-scale, versatile computer codes.

One of the codes, TRACER (22), has been used to study the effect of a large, poorly fragmented block of material inside an *in situ* oil shale retort. Of particular interest is the effect this block has on tracer flow measurements that might be made to remotely diagnose the internal state of the retort. The retort geometry and the locations within it of six tracer gas sampling stations are shown in Fig. 9. The poorly fragmented block is represented as a region of reduced permeability in the upper right hand corner of the retort. The tracer gas (argon in this case) is injected in a short pulse at the top. The calculated tracer gas concentrations at sampling stations

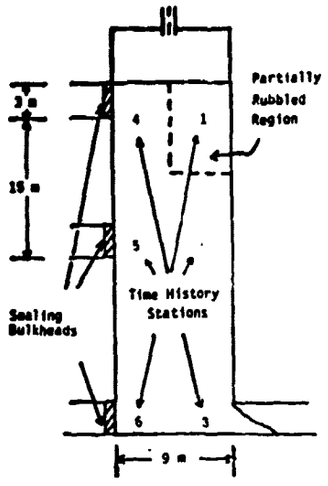

Fig. 9 Schematic diagram of an *in situ* oil shale retort. The "partially rubbled region" in the upper right is assumed to have a much lower permeability than the rest of the retort. The tracer gas is introduced at the top of the retort and is sampled at the six labeled "time history stations." Gas is permitted to exit at the bottom of the retort on the right side.

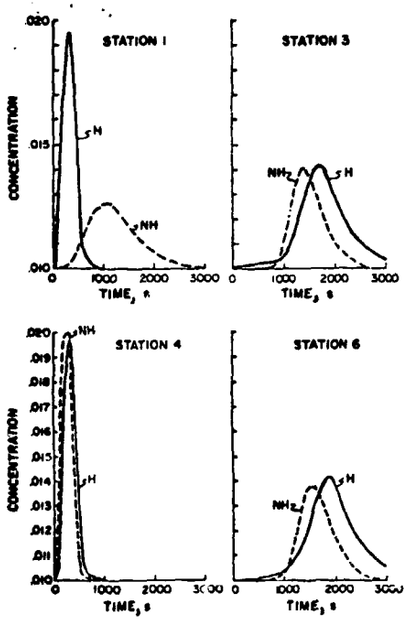

Fig. 10 Time histories of tracer gas (concentration by weight versus time) at four of the sampling stations in the oil shale retort shown in Fig. 9. The curves marked "NH" are for a retort with a partially rubbled region, as in the retort in Fig. 9; the curves marked "H" are for a uniformly rubbled homogeneous retort for comparison. The tracer measurements at station 1 are quite sensitive to the presence of the poorly rubbled region. However, dispersion within the retort causes the measurements at the other stations to be rather insensitive to the state of the retort for the assumed pulse duration and gas flow rate.

1, 3, 4, and 6 are shown as functions of time in Fig. 10. Curves are shown for the inhomogeneous retort with the block (labeled "NH") and for a homogeneous retort with uniform permeability (labeled "H") for comparison.

The curves in Fig. 10 show that the tracer and mass flow through the low permeability block at the top of the retort are inhibited relative to the flow in the homogeneous retort. The calculations also show, however, that significant dispersion occurs in the retort, so that the tracer curves at the bottom of the retort are almost the same for the inhomogeneous and homogeneous retorts. Calculations such as these will be essential for planning tracer sampling strategies for *in situ* fragmentation diagnostic techniques.

Another code, KRAK (23), has been developed to model the extension of a new or existing fracture being driven by a high pressure gas. The gas may be condensible (e.g., steam) or even reactive (e.g., a slow-burning propellant). The code allows for visco-inertial flow in the crack and for flow from the crack into a medium of variable porosity, permeability, and saturation level. The common assumption of Darcy's Law is not made in the code. Some results obtained with the KRAK code are shown in Fig. 11. There the growth of crack length with time is shown for several assumed permeabilities for the surrounding medium. The rate of crack growth clearly depends sensitively on the rate at which the flow can diffuse away from the crack. This effect can have a pronounced influence on wellbore springing applications.

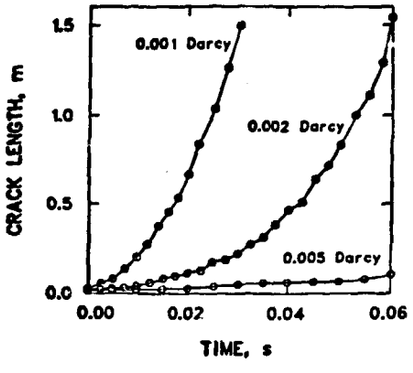

Fig. 11 Crack length versus time for several assumed permeabilities for the surrounding medium. Note how increased permeability allows diffusion away from the crack and greatly inhibits the rate of crack growth. The actual growth rates depend on the driving force and the material properties of the medium. Conversion factor: (Darcy) = (1.8697×10^{-13}) (m^2).

These examples illustrate the progress that has been made toward the description and modeling of fluid flow in geologic materials. Related modeling techniques can be used to described the dewatering of a coal seam, reactive coal gasification schemes, and gas flow in a reservoir. It is important to emphasize, though, that we have just begun to understand this enormously complex problem.

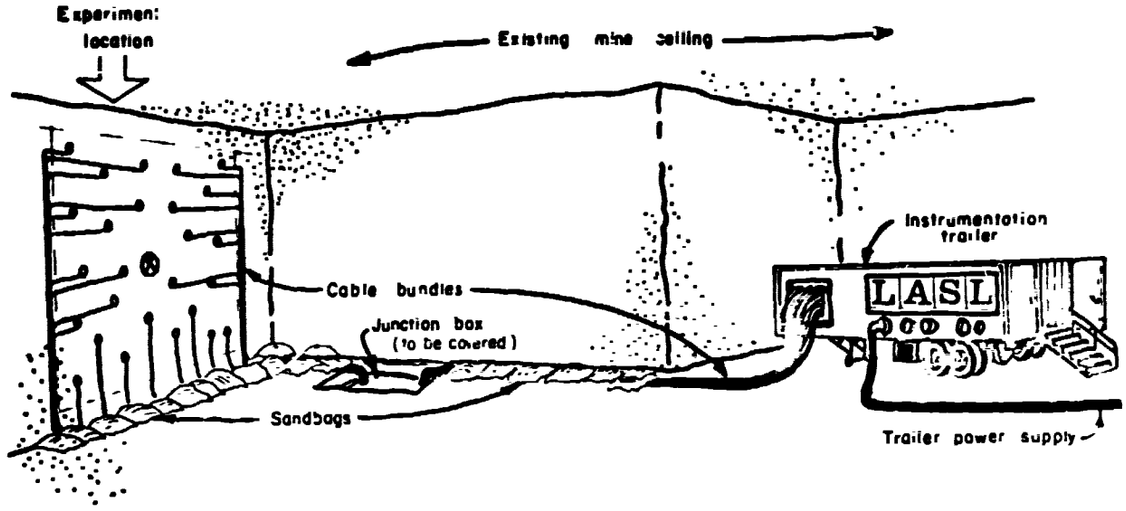

Fig. 12 Typical arrangement for a field experiment to study explosive rubbling of oil shale. In this sketch, the explosive borehole (circle marked with a cross) is drilled horizontally, parallel to the bedding planes. (The firing cable is not shown here). The shot hole is surrounded by diagnostic holes, in which stress and accelerometer gauges have been deployed. Data recording is done in real time during the blast in the on-site instrumentation trailer.

FIELD TESTS

The ability to design fragmentation methods to achieve permeability enhancement suitable for georesource recovery can only be verified by comparing calculational results with large-scale, heavily instrumented explosive field tests. Past experience has demonstrated that predictions based on simple concepts or traditional methods do not always yield satisfactory results in the field. The number of variables to be considered is large and isolation of key parameters is an extremely difficult task. Observations necessary for direct comparison with calculations are stress wave profiles, particle velocity and acceleration measurements, free surface motion, and post-shot determination of fragmentation results. In order to determine the effects of geophysical variables such as bedding plane orientation, hydrocarbon content, and joint and fracture spacing, an extensive preshot examination of the test region is also required. Very few such quantitative tests have been performed.

Examples of the type of experiments needed on large-scale blasting effects are the oil shale bed preparation studies being conducted by the Los Alamos Scientific Laboratory. The geometry for one of these experiments, a single explosively-loaded borehole parallel to the bedding plane, is shown in Fig. 12. Surrounding the explosive borehole are numerous diagnostic holes containing stress gauges and accelerometers. A series of these experiments is in progress at the Colony Mine near Rifle, CO. These experiments are being performed under DOE auspices with the cooperation of Atlantic Richfield, TOSCO, and the Colony Development Corporation.

Predictions for the stress history at a gauge location about 1 m from the explosive borehole for one of the recent field experiments are shown in Fig. 13. The calculated peak stress for this gauge is in good agreement with the preliminary data for this experiment (24). This confirmation of the accuracy of the calculations is quite encouraging. Efforts to predict the distribution of rock breakage around the borehole and the effects of decked charges in a single borehole are presently underway.

Because the success of large-scale field tests, especially those involving multiple boreholes, is crucially dependent on the behavior of the explosive, pulsed time delay reflectometers (25) employing low crush cables are deployed in the borehole to monitor the explosive detonation behavior. The value of these

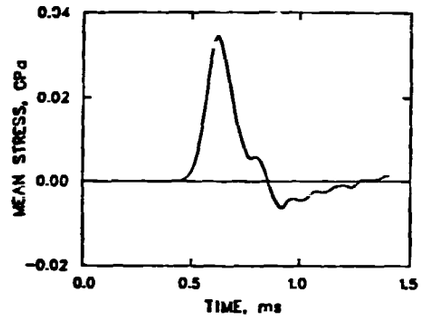

Fig. 13 Calculated mean stress versus time for a gauge located approximately 1 m away from a 108 mm diameter charge of ANFO. This calculation was made in connection with a recent field test in oil shale. The preliminary observed peak stresses for three gauges at this range in the experiment were 0.03, 0.05, and 0.07 GPa (24), in reasonable agreement with the calculations. The scatter in the data probably reflects the importance of the local geology (e.g., presence of pre-existing joints).

measurements can be seen in Fig. 14. In this experiment, the cap and booster were near the bottom of the borehole. The abrupt jump in the data show that the booster was not precisely at the bottom. In fact, the explosive was initiated a small distance away from the bottom of the hole. Without knowledge of exactly how the explosive performed, the stress wave and accelerometer data would have been extremely difficult to interpret.

Post-shot diagnostics are now being performed for this series of experiments, including post-shot coring, acoustic mapping, tracer flow measurements, and excavation of the fragmented region. These measurements will be used to characterize the fragmentation results so that the permeability distribution can be directly connected to the explosive loading. These experiments are difficult and costly. However, the potential payoff of improved permeability enhancement techniques through better blast control and the increase in our understanding of basic explosive processes is so great that this extra effort is fully warranted.

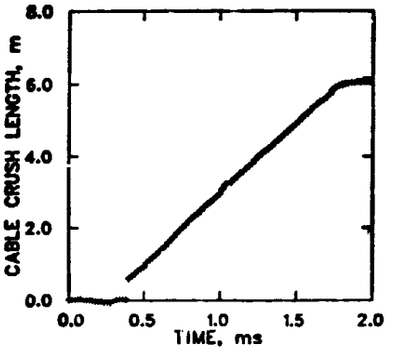

Fig 14 Cable crush length versus time for a CORRTEX diagnostic cable deployed inside a 150 mm diameter borehole loaded with ANFO. The crush length increases from zero as the detonation front runs up the 6 m long borehole. The detonation velocity can be measured quite accurately from the slope of the length-time data. The abrupt jump from zero shows that the detonator was located a short distance above the bottom of the borehole.

ACKNOWLEDGMENT

This work was performed under the auspices of the US Department of Energy, Division of Fossil Fuel Extraction.

REFERENCES

1 Blasters' Handbook, 175th ed., E. I. du Pont de Nemours and Co., Wilmington, 1977, pp. 1-18.

2 Harlow, F. H., and Amsden, A. A., "Fluid Dynamics," LA-4700, June 1971, University of California, Los Alamos Scientific Laboratory, Los Alamos, NM.

3 Craig, B. G., Johnson, J. N., Mader, C. L., and Lederman, G. F., "Characterization of Two Commercial Explosives," LA-7140, May 1978, University of California, Los Alamos Scientific Laboratory, Los Alamos, NM.

4 Mader, C. L., Numerical Modeling of Detonations, University of California Press, Berkeley, 1979.

5 Carter, W. J., "Hugoniots of Green River Oil Shale," in "Explosively Produced Fracture of Oil Shale, Annual Report, March 1976 - March 1977," LA-6817-PR, Sept. 1977, University of California, Los Alamos Scientific Laboratory, Los Alamos, NM, pp. 2-6.

6 Olinger, B., "Oil Shales under Dynamic Stress," in "Explosively Produced Fracture of Oil Shale, April 1977 - March 1978," LA-7357-PR, Nov. 1978, University of California, Los Alamos Scientific Laboratory, Los Alamos, NM, pp. 2-10.

7 Johnson, J. N., and Simonson, E. R., "Analytical Failure Surfaces for Oil Shale of Varying Kerogen Content," in Timmerhaus, K. D., and Barber, M. S., eds., High-Pressure Science and Technology, Sixth AIRAPT Conference, Vol. 2, Plenum Press, New York, 1979, pp. 444-454.

8 Olinger, B., private communication.

9 Carter, W. J., Olinger, B. W., Vanderborgh, N. E., and Springer, T. E., "Gas Stimulation Studies at LASL," Proceedings of ERDA Enhanced Oil, Gas Recovery and Improved Drilling Methods, Petroleum Publishing Co., Tulsa, 1977, pp. F1/1-F1/17.

10 Smith, J. W., "Specific Gravity-Oil Yield Relationships of Two Colorado Oil Shale Cores," Industrial and Engineering Chemistry, Vol. 48, No. 3, Mar. 1956, pp. 441-444.

11 Olinger, B., "Elastic Constants of Oil Shale," in "Explosively Produced Fracture of Oil Shale, Annual Report, March 1976 - March 1977," LA-6817-PR, Sept. 1977, University of California, Los Alamos Scientific Laboratory, Los Alamos, NM, pp. 24-26.

12 Olinger, B. W., "Dynamic Properties of Devonian Shales," in "Evaluation of Methods and Characterization of Eastern Gas Shales, April - June 1977," LA-7094-PR, Jan. 1978, University of California, Los Alamos Scientific Laboratory, Los Alamos, NM, pp. 1-10.

13 Johnson, J. N., "Calculation of Explosive Rock Breakage: Oil Shale," Proceedings of the 20th U.S. Symposium on Rock Mechanics, U.S. National Committee for Rock Mechanics, June 1979, pp. 109-118.

14 McQueen, R. B., Marsh, S. P., and Fritz, J. N., "Hugoniot Equation of State for Twelve Rocks," Journal of Geophysical Research, Vol. 72, No. 20, 15 Oct. 1967, pp. 4999-5036.

15 Young, C., and Powell, C. N., "Lateral Inertia Effects on Rock Failure in Split-Hopkinson-Bar Experiments," Proceedings of the 20th U.S. Symposium on Rock Mechanics, U.S. National Committee for Rock Mechanics, June 1979, pp. 109-118.

16 Lankford, J., "Dynamic Strength of Oil Shale," Society of Petroleum Engineers Journal, Vol. 16, No. 1, Feb. 1976, pp. 17-22.

17 Kuznetsov, V. M., and Faddeenkov, N. N., "Fragmentation Schemes," Combustion, Explosion, and Shock Waves, Vol. 11, No. 4, July - Aug. 1975, pp. 541-548.

18 Butkovich, T. R., "Correlations between Measurements and Calculations of High-Explosive-Induced Fracture in a Coal Outcrop," International Journal of Rock Mechanics and Mining Science and Geomechanics Abstracts, Vol. 13, No. 2, Feb. 1976, pp. 45-51.

19 Grady, D. E., and Kipp, M. E., "Continuum Fracture and Fragmentation of Rock: Application to Oil Shale," SAND78-1282, July 1978, Sandia Laboratories, Albuquerque, NM.

20 McHugh, S. L., Seaman, L., Murri, W. J., Tokheim, R. E., and Curran, D. R., "Fracture and Fragmentation of Oil Shale," Final Report on SRI Project PYD-6128, Dec. 1977, SRI International, Menlo Park, CA.

21 Dienes, J. K., and Margolin, L. G., in "Explosively Produced Fracture of Oil Shale," Quarterly Progress Reports for July - September 1978 and October - December 1978, to be published.

22 Travis, B. J., "Gas Flow Calculations for Proposed Rio Blanco Oil Shale Company Retort," in "Explosively Produced Fracture of Oil Shale, October - December 1978," to be published.

23 Davis, A. H., and Travis, B. J., "KRAK: A Computer Program for Two-Phase, Two-Component Porous Flow and Fracture," to be published.

24 R. Reed, Sandia Laboratories, Albuquerque, NM, private communication.

25 McKown, T. O., Goldwire, H. C., Eilers, D. D., and Honey, F. J., "ANFO Detonation Velocity Measurements for Colony Mine Experiments," "Explosively Produced Fracture of Oil Shale, April - June 1979," to be published.